



ELSEVIER

Available online at [www.sciencedirect.com](http://www.sciencedirect.com)

SCIENCE @ DIRECT®

Optics and Lasers in Engineering 44 (2006) 1239–1251

---

---

OPTICS and LASERS  
in  
ENGINEERING

---

---

# Objective evaluation of information retrieved from digitally compressed in-line holograms

Joewono Widjaja\*

*Institute of Science, Suranaree University of Technology, Nakhon Ratchasima 30000, Thailand*

Received 1 November 2004; received in revised form 1 August 2005; accepted 1 December 2005

Available online 10 March 2006

---

## Abstract

Quality of information retrieved from digitally compressed in-line holograms are objectively studied by evaluating the measured recording distance and its reconstructed image. A lossy-JPEG algorithm is used for compression of the in-line Fraunhofer holograms, while the information retrieval is accomplished by using complex amplitude based numerical reconstruction method. The results show that the error in measurement of recording distance and the degradation of the reconstructed image are not significant although the hologram is compressed by about 60 times. This provides a practical solution to the storage and data transfer problems in on-line digital in-line holography.

© 2006 Elsevier Ltd. All rights reserved.

*Keywords:* In-line Fraunhofer holography; Particle sizing; Image compression

---

## 1. Introduction

In the past decades, applications of in-line Fraunhofer holography to the fields of science and engineering such as studies of dynamic micro-objects [1], fog [2], aerosol [3], cloud droplets [4], oceanic particles [5], and bio-stabilized sediments [6] have been reported. The technique provides a useful method for storing information, size and relative position, of a three-dimensional (3-D) distribution of objects in holographic

---

\*Tel.: +66 44 224194; fax: +66 44 224185.

E-mail address: [widjaja@sut.ac.th](mailto:widjaja@sut.ac.th).

plate. In the in-line Fraunhofer holography, opaque or semi-transparent objects are illuminated by a collimated coherent light. By recording an interference pattern produced between light waves diffracted from the objects and the light wave transmitted directly onto photosensitive media such as holographic film, a hologram of the objects is generated. In order to study the objects rigorously, the developed hologram is re-illuminated by the same coherent light. The stationary image of the object is reconstructed at the same distance as the recording distance. Since, in general, this distance is not known in advance, the image plane of best focus for each object must be investigated by scanning the overall depth along an optical axis with fine steps. Since the conventional reconstruction process is very tedious and time consuming, computer-based algorithm is employed to perform automatic analysis and measurement.

With current technological development of charge-coupled device (CCD) image sensors, it is possible to record directly the interference patterns by the sensors, yielding digital holograms. The digital holography has several advantages over the conventional ones in that it is free from wet chemical development and no optical reconstruction is needed. In comparison with the off-axis configuration, the in-line holography can be easily accomplished by using the CCD sensors, because its configuration does not have stringent spatial-resolution requirement on the sensors [7]. In the digital holography, the stored information can be digitally retrieved by using either numerical reconstruction [8–10] or signal processing approach [11,12]. In the case of the numerical reconstruction method, the amplitude and phase of the objects can be obtained by solving a Fresnel diffraction integral of the digitized holograms at consecutive depth along the optical axis. From the numerical standpoint, the diffraction integral can be solved either by convolving the digitized holograms with the Fresnel diffraction kernel or by calculating a discrete Fresnel transform. Since searching for the best depth position is still required, the numerical reconstruction method also suffers from long computational time. On the other hand, when the real image of the objects is not of particular interest, the signal processing approach that employs either a Wigner distribution function or wavelet transform can be used for extracting directly the spatial position and size of the objects from the holograms. Since this approach does not require the knowledge of the correct position of the in-focus plane, the processing time can be significantly reduced.

Although the spatial resolution requirement on the CCD sensors is relaxed, information retrieval from the digital in-line holography will be faithfully done provided the spatial resolution and the number of pixels of the CCD sensor is sufficient to sample the interference fringes. This leads to the use of the CCD sensor with mega pixel resolution producing a large file size of the digital hologram. Since in practice we may have to deal with a large number of in-line digital holograms, the digital in-line holography requires considerable storage capacity. Furthermore, in the case of remote sensing, the captured digital holograms may have to be electronically transferred from remote locations or hostile environments to a host computer for analysis. To perform on-line analysis, a transmission network with

high bandwidth and data transfer rate is required. However, this may lead to an expensive system.

In order to solve these problems, we envision a use of a lossy-image compression such as a joint-photographic experts group (JPEG) [13] to reduce the file size of the digital holograms. This interest stems from the result of our previous study of compression of digital specklegrams which reveals that the specklegrams can be compressed into the JPEG format by manifolds without distorting significantly displacement information [14]. Note that the JPEG format is widely supported by commercially available CCD sensors.

In the JPEG algorithm, the image distortion occurs because the compression is achieved by discarding permanently image details through a series of processing steps that are [13]: First, the digital image is grouped into  $8 \times 8$  pixel blocks. Second, a discrete cosine transform (DCT) is applied to each block for providing 1 dc and 63 ac frequency components. Third, each of the 64 frequency components is quantized according to a designed 64-element quantization table. In this step, each frequency component is divided by a corresponding number from the particular element of the quantization table and then is rounded to the nearest integer. Since human eye is less sensitive to high-frequency details than to low-frequency ones, the high-frequency components normally are divided by larger coefficient than the lower one. As the result most ac components are zeros. This is the step where information is irretrievably lost. Finally, the non-zero and the zero-frequency components are encoded by using a combination of a Huffman coding and a run length encoding in order to achieve efficient compression.

For the preceding reasons, it is important to study feasibility of compressing the in-line Fraunhofer holograms by using the JPEG algorithm. The study is conducted by evaluating quantitatively the quality of the measured recording distance and the reconstructed image from the compressed holograms obtained by using the complex amplitude based numerical method.

## 2. Theory

### 2.1. In-line holography

Consider a particle with an amplitude transmittance function  $O(\xi, \eta)$  is illuminated by a unit-amplitude plane wave with wavelength  $\lambda$ . The field distribution at the recording plane a distance  $z$  away can be mathematically expressed as [1]

$$\Psi(x, y) = [1 - O(x, y)] \otimes h_z(x, y), \quad (1)$$

where  $\otimes$  denotes convolution operation, while  $h_z(x, y)$  is the Fresnel diffraction kernel given by

$$h_z(x, y) = \frac{\exp(ikz)}{i\lambda z} \exp\left[\frac{ik}{2z}(x^2 + y^2)\right]. \quad (2)$$

By recording this field distribution  $\Psi(x, y)$ , the amplitude transmittance of the hologram is proportional to the intensity distribution

$$I(x, y) = 1 + |O(x, y) \otimes h'_z(x, y)|^2 - O(x, y) \otimes h'_z(x, y) + O^*(x, y) \otimes h'^*_z(x, y) \quad (3)$$

with

$$h'_z(x, y) = \frac{1}{i\lambda z} \exp\left[\frac{ik}{2z}(x^2 + y^2)\right]. \quad (4)$$

The first and the second terms of Eq. (3) represent the directly transmitted light and intermodulation term which can be neglected because its amplitude is much smaller compared with the other terms [15]. The third term corresponds to the virtual image, while the last term is of particular interest since it can be used to generate real image of the particle distribution.

In the optical reconstruction, the hologram is illuminated by the same collimated coherent light. When the reconstruction distance is set to be exactly equal to the recording distance, the reconstructed field is found to be

$$\begin{aligned} \phi(x, y) &= I(x, y) \otimes h_z(x, y) \\ &= 1 - O(x, y) \otimes h'^*_z(x, y) + O^*(x, y). \end{aligned} \quad (5)$$

Here the constant phase factor of the kernel and the second term of Eq. (3) are neglected. The first two terms can be regarded as the field of the hologram of the same particle recorded at a distance  $2z$ , while the third term is the reconstructed image of the particle. Due to a nature of a square law detector, the reconstructed image is proportional to the intensity  $|O^*(x, y)|^2$ .

## 2.2. Numerical reconstruction

In order to perform numerical reconstructions, the digital holograms are generated by either recording directly the interference pattern by using the CCD sensor or scanning digitally the developed holographic films. The digital holograms are then convolved with the kernel  $h'_z(x, y)$  of Eq. (4). As a result instead of intensity, the numerical computation of Eq. (5) gives the complex amplitude of the wave field  $O^*(x, y)$  of the image particle [8].

It is worth mentioning that for opaque particle, the field  $O(\xi, \eta)$  or its conjugate  $O^*(\xi, \eta)$  can be mathematically described by a real function. Therefore by taking this fact into account, the amplitude of the image field does not contain any imaginary value provided the reconstruction distance is exactly equal to the recording distance [10]. However, due to contribution of the other terms in Eq. (5) which may have complex value, it is hard to detect only the real part of the amplitude of the image field. In order to obviate this problem, the variance of the imaginary part of the complex amplitude  $\phi(x, y)$  has been used for determining the correct axial position of particles by Pan et al. [10]. According to this technique, the variance of the imaginary part of the amplitude  $\phi(x, y)$  is minimum when the axial position matches

to the recording distance, because the image field is real. In unmatched case, the variance increases.

### 2.3. JPEG compression

In the JPEG algorithm, the compression is started by grouping picture elements of the input image into  $8 \times 8$  pixel blocks. The encoding process is achieved through three-step processes. In the first encoding step, the spatial frequency  $S(u, v)$  of each block  $s(x, y)$  is independently calculated by using the 2-D DCT given by [13]

$$S(u, v) = \frac{C(u)C(v)}{4} \sum_{x=0}^7 \sum_{y=0}^7 s(x, y) \cos\left\{\frac{(2x+1)u\pi}{16}\right\} \cos\left\{\frac{(2y+1)v\pi}{16}\right\}, \quad (6)$$

where

$$C(u) = \begin{cases} 1/\sqrt{2} & \text{for } u = 0 \\ 1 & \text{for } u > 0 \end{cases} \quad \text{and} \quad C(v) = \begin{cases} 1/\sqrt{2} & \text{for } v = 0 \\ 1 & \text{for } v > 0. \end{cases}$$

The transformation produces spatial frequencies consisting of 1 dc and 63 ac frequency coefficients. Tables 1(a) and (b) show the  $8 \times 8$  pixel values of one block of the image and its DCT coefficients, respectively. The dc coefficient appears at the top left corner of Table 1(b), while the ac coefficients are the remaining numbers. The spatial frequency becomes higher as the position of the ac coefficient goes to the bottom right corner. Since the pixel values of the image vary slowly, the value of the dc coefficient is larger than that the ac ones. In the second step, the resultant DCT of each block is quantized by dividing each value of the DCT coefficient by a corresponding number from a quantization table. In order to discard high spatial-frequency contents, the quantization value for the dc coefficient is set to be smaller than that of the ac ones. Table 1(c) shows the default quantization for luminance of grayscale images whose values increase from the top left corner to the bottom right one. The quantized DCT coefficient is then rounded to the nearest integer. Table 1(d) shows the resultant integer values where most ac coefficients become zeros. To prepare further compression, the resultant  $8 \times 8$  coefficients are rearranged into a 1-D linear array of  $1 \times 64$  values with order of increasing spatial frequency. In the final step, the dc coefficient is processed by storing the difference between dc coefficients of consecutive blocks. As for the ac coefficients which consist of sequential zero values, the compression is achieved by using the run length encoding and the Huffman coding. If there are  $n$  consecutive occurrences of datum 0 in the array, the run length encoding compresses this sequence by representing the  $n$  consecutive occurrences as  $n0$ . The output of the run length encoding is further compressed by using the Huffman coding. However unlike the run length encoding, this compression is based on the fact that certain datum of the input sequence occurs more frequent than others. Thus, the compression is achieved by employing probability of occurrence of each datum where a shortest binary code is assigned to the most frequent datum, while the longest one is for the least frequent one.

Table 1  
JPEG encoding process

(a) Pixel values of $8 \times 8$ image block							
55	73	103	66	55	50	68	71
62	97	58	55	63	66	78	63
52	54	49	50	58	83	65	67
53	51	47	47	45	43	66	52
52	59	55	50	49	44	57	52
50	61	72	50	46	53	47	55
55	63	85	57	46	47	49	50
52	48	71	54	45	48	49	55
(b) Its DCT coefficients							
461.37	9.24	10.54	-26.47	-28.37	-1.13	2.26	7.94
37.70	-13.65	7.88	8.087	-8.50	-7.60	-16.49	-3.39
28.57	14.49	-6.70	-23.85	-8.15	-0.55	10.41	6.56
8.13	21.08	-3.72	-26.25	-6.33	-1.54	2.52	9.30
-15.12	1.33	0.93	-14.27	8.62	13.75	-1.33	11.36
-4.46	2.34	-5.15	-13.22	0.40	10.72	12.74	7.75
-3.85	-14.25	-6.34	-0.70	3.51	0.18	20.70	-2.31
4.16	-4.08	-6.41	-0.06	1.51	-0.06	9.24	-0.82
(c) Quantization table							
16	11	10	16	24	40	51	61
12	12	14	19	26	58	60	55
14	13	16	24	40	57	69	56
14	17	22	29	51	87	80	62
18	22	37	56	68	109	103	77
24	35	55	64	81	104	113	92
49	64	78	87	103	121	120	101
72	92	95	98	112	100	103	99
(d) The quantized coefficients of Table 1(b)							
29	1	1	-2	-1	0	0	0
3	-1	1	0	0	0	0	0
2	1	0	-1	0	0	0	0
1	1	0	-1	0	0	0	0
-1	0	0	0	0	0	0	0
0	0	0	0	0	0	0	0
0	0	0	0	0	0	0	0
0	0	0	0	0	0	0	0

### 3. Results and discussions

In order to study the effects of compression on the desired information, the in-line holograms of an optical fiber with a radius  $a$  of  $62.48 \mu\text{m}$  were generated at the recording distance  $z$  of 9 and 19 cm by using a laser light operating at a wavelength of 543.5 nm. The optical fiber was oriented along the vertical direction and its interference pattern was captured by the Hamamatsu C5948 CCD camera with the resolution of  $640 \times 480$  pixels in the area of  $8.3 \times 6.3$  mm. The recorded holograms were saved by using the Hamamatsu LEPAS-11 image processing software in TIFF

file format with a pixel depth of 24 bits. The size of each digital hologram was about 904 Kbytes. Figs. 1(a) and (b) shows the digital holograms of the optical fiber recorded at the distances  $z$  of 9 and 19 cm, respectively. The transmittance function of these holograms can be approximately expressed as

$$I(x) = 1 - \frac{4a}{\sqrt{\lambda z}} \cos\left(\frac{\pi x^2}{\lambda z} - \frac{\pi}{4}\right) \left[\frac{\sin(2\pi ax/\lambda z)}{2\pi ax/\lambda z}\right]^2, \quad (7)$$

which consists of a modulation of a chirp signal by a sinc function. In Eq. (7), the frequency of the chirp signal is proportional to  $x/\lambda z$ , while the zero-crossing positions of the sinc function are determined by a factor  $\lambda z/2a$ . By taking these factors into account, for the long recording distance  $z$ , the sinc function becomes broad and the frequency of the chirp signal increases slowly. This can be clearly observed from Fig. 1 which shows that in comparison with Fig. 1(a) the size of the interference pattern in Fig. 1(b) is approximately two times broader and its fringe spacing decreases slower. Furthermore, when the spatial position  $x$  increases, the spatial frequency of the chirp signal will eventually become higher than the sampling frequency of the CCD sensor. As the fringe spacing becomes finer, the fringes in the higher-order side lobes of the sinc function are under-sampled, aliasing error occurs in which the higher frequencies of the chirp signal are detected as lower frequencies [16]. As a consequence, Fig. 1(a) shows that only the fringes around the main lobe of the sinc function can be clearly observed because they are faithfully sampled by the CCD sensor. Since the aliasing error occurs at the higher-order side lobes, it is hard to observe its fringes. In contrast, it is obvious that the amplitude variation of the fringes up to the first-order of the side lobe can be observed from Fig. 1(b). Since less fringes are affected by the aliasing error, the hologram recorded at the distance  $z = 19$  cm contains more high spatial-frequency components.

The digital holograms were then compressed into the JPEG file format by using ACDsee software version 3.1. In this software, the compression quality is determined by a parameter called the quality factor (QF) whose value can be varied from 100 to 0. High value of the QF discards less information than that of the small value. Thus,

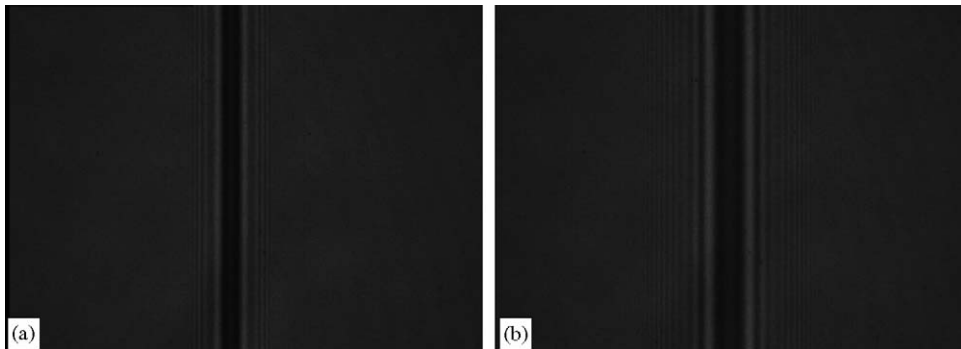


Fig. 1. In-line holograms of optical fiber recorded at distance (a) 9 cm, and (b) 19 cm, respectively.

the higher the value of the QF, the better the image quality and bigger the file size of the compressed image. As a function of the QF of the holograms, Fig. 2 shows the compression ratio (CR) and the bit rate (BR) which are represented by the solid and the dash lines, respectively. The CR is defined as the ratio of the uncompressed file size to the compressed file size, while the BR is the average number of compressed bits/pixel [13]. By decreasing the QF, the average number of bits BR used to represent each pixel becomes lower. As a consequence, the value of the CR becomes higher. It is clear from Fig. 2 that for the same value of the BR, the CR of the hologram recorded at the distance  $z = 9\text{ cm}$  is higher than that of the hologram recorded at 19 cm, because the aliasing error reduces more high spatial-frequency components of the hologram recorded at a shorter distance. The quantization process done on this hologram yields more zeroes of the ac components. As a consequence, the run length coding and the Huffman coding can encode efficiently the redundant zeroes.

In this work, the lowest QF produced the compressed file of 4 Kbytes, while the highest QF gave about 141 Kbytes. The compressed holograms corresponding to Figs. 1(a) and (b) with  $QF = 50$  are shown in Figs. 3(a) and (b), respectively. It is obvious that it is hard to observe the effect of compression on the digital holograms.

The compressed holograms were numerically reconstructed by convolving their transmittance function with the Fresnel diffraction kernel  $h_z(x, y)$ . All computations were conducted by using the Matlab 6.1. In order to find the correct recording distance, the variance of the imaginary part of the complex amplitude  $\phi(x, y)$  is investigated at consecutive depth  $z$  along the optical axis. When the variance is

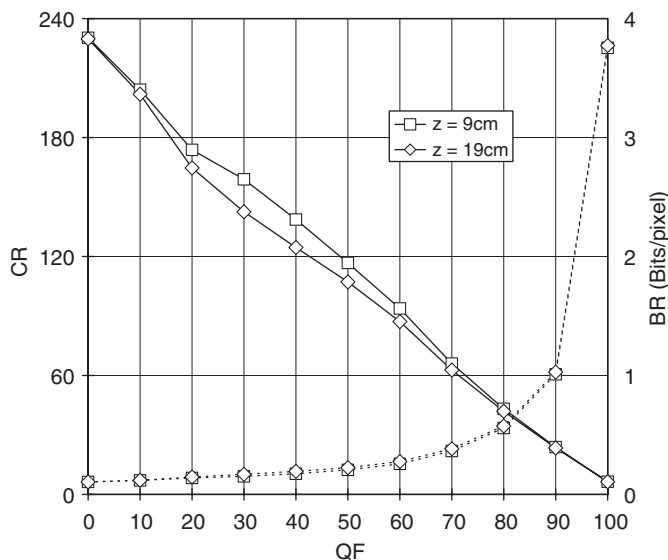


Fig. 2. Compression ratio (CR) and bit rate (BR) of the compressed in-line holograms as a function quality factor (QF).

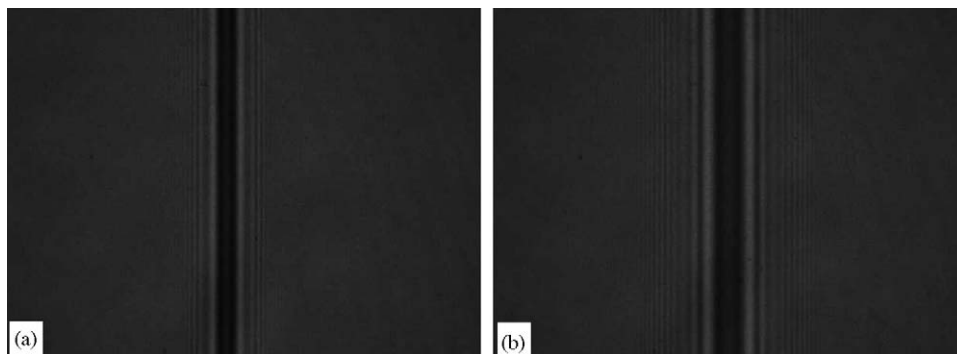


Fig. 3. Compressed in-line holograms recorded at distance (a) 9 cm, and (b) 19 cm with  $QF = 50$ , respectively.

minimum, the reconstruction distance  $z$  employed in the Fresnel diffraction kernel  $h_z(x, y)$  can be regarded as the correct recording distance. In fact, this approach is equivalent to searching the in-focus image plane of particles reconstructed from the hologram.

The first objective evaluation is to calculate the error in measurement of the recording distance from the compressed in-line holograms. The error was calculated by comparing its measured distance with the resultant value obtained from the corresponding original hologram. Fig. 4 shows the error of the measured distance  $z$  as a function of the  $QF$  for the holograms recorded at two different distances. In general, the error increases as the  $QF$  decreases, because more image information is discarded from the compressed holograms. However, in the case of the compressed hologram recorded at the distance  $z = 9$  cm, the error and its rate of change are higher than that of the holograms recorded at 19 cm. As discussed before, the hologram recorded at shorter distance can be efficiently compressed than the holograms recorded at longer distance, because for the same value of the  $QF$ , more fine detail of the fringes is discarded. Since the degradation of the fringes is more significant, the error in measurement of the recording distance becomes higher.

Figs. 5(a) and (b) illustrates the images of the fiber reconstructed from the original holograms recorded at the distance  $z = 9$  and 19 cm, respectively. Whereas the reconstructed images from the corresponding compressed holograms with the  $QF = 70$  are illustrated in Figs. 5(c) and (d). In comparison with Fig. 5(a), the reconstructed image from the original holograms recorded at the distance  $z = 19$  cm shows better quality, because the aliasing error of the hologram recorded at a long distance is less severe. For  $QF = 70$  which is corresponding to the compression of about 60 times with its BR of about 0.2 bits/pixel, the figures show that regardless of the recording distance, the degradation of the reconstructed images from the compressed hologram cannot be observed. This subjective evaluation reveals that the effect of compression is insignificant.

In order to study further the effect of compression on the compressed holograms, the quality of the reconstructed images is quantified by using the mean square error

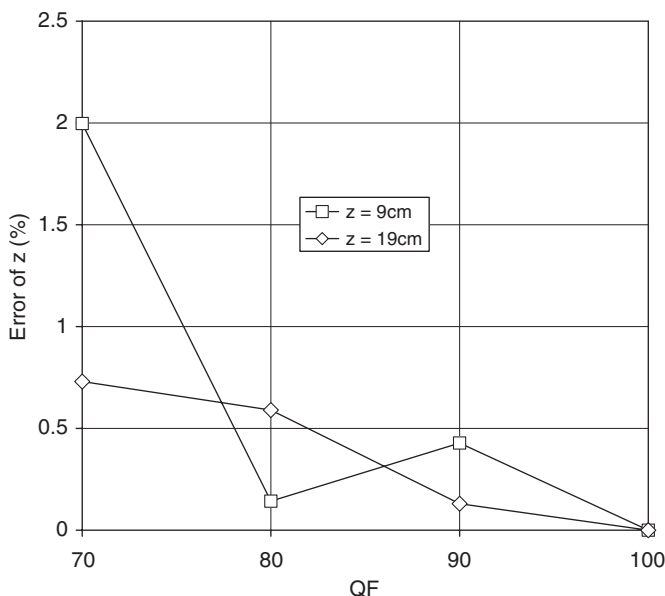


Fig. 4. Error in measurement of recording distance as a function of QF for compressed holograms with recording distances 9 and 19 cm.

(MSE) given by [17]

$$\text{MSE} = \frac{1}{M \times N} \sum_{m=1}^M \sum_{n=1}^N [f(m, n) - f'(m, n)]^2, \quad (8)$$

where  $f(m, n)$  and  $f'(m, n)$  stand for the original and its compressed image files, respectively. In the image compression, the MSE which is used widely for objective image evaluation measures the difference between the original and the compressed images. A large MSE means that the degree of difference between the original image and its compressed versions is high. The MSE was computed for each reconstructed image from the compressed holograms. Fig. 6 shows the variation of the MSE as a function of the QF for the compressed holograms recorded at two different distances. It is clear that the MSE and its rate of change are small for the compressed hologram recorded at the distance  $z = 19$  cm than that of the hologram with shorter distance of 9 cm. Thus the image of the optical fiber can be faithfully reconstructed from the compressed hologram recorded at longer distance. This is in a good agreement with the error in measurement of the recording distance shown in Fig. 4, because the reconstruction process done at the erroneous distance  $z$  produces unfaithful image. Thus, the higher the error, in measurement of the recording distance, the larger the MSE.

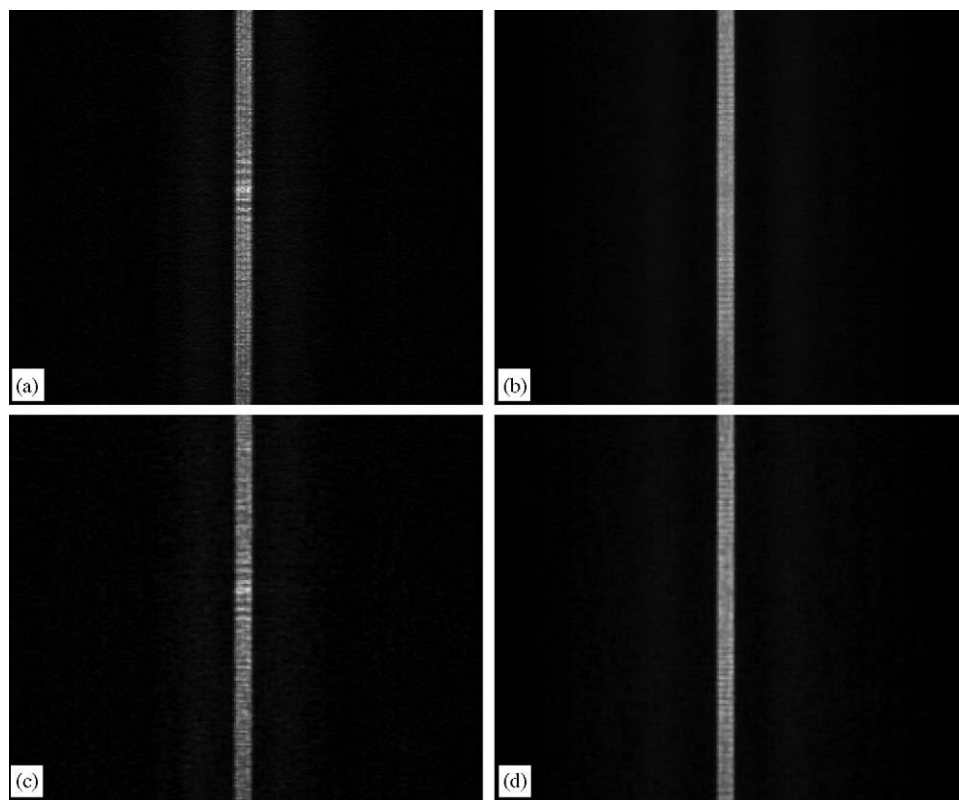


Fig. 5. Reconstructed images from original holograms recorded at distance (a) 9 cm, (b) 19 cm, and from the compressed holograms recorded at distance (c) 9 cm, and (d) 19 cm with  $QF = 50$ , respectively.

The preceding results show that the compression of the hologram recorded at  $z = 19$  cm by 60 times causes only 0.7% error of recording distance and does not degrade the reconstructed image. As for the hologram recorded at the shorter distance, the effects of compression are more severe. This is mainly caused by the limited resolution of the CCD sensor which cannot sample narrow fringes of the interference pattern generated at a short recording distance.

#### 4. Conclusions

We have evaluated objectively quality of the information retrieved from the JPEG-compressed in-line holograms by using the numerical approach. The effects of compression on the retrieved information are found not significant provided the resolution of the CCD sensor is sufficient to sample the interference fringes. This result provides practical solution to the storage and the data transfer problems in the on-line digital in-line holography.

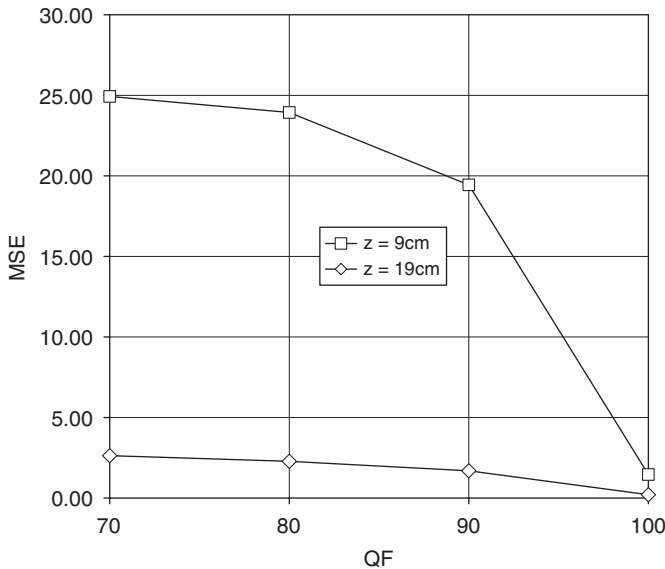


Fig. 6. MSE as a function of QF for compressed holograms with recording distances 9 and 19 cm.

## Acknowledgement

This work was supported by the SUT Research Grant 2544.

## References

- [1] Tyler GA, Thompson BJ. Fraunhofer hologram applied to particle analysis: a reassessment. *Optica Acta* 1976;23:685–700.
- [2] Thompson BJ. Holographic particle sizing technique. *J Phys E* 1974;E7:781–8.
- [3] Grabowski W. Measurement of the size and position of aerosol droplets using holography. *Opt Laser Technol* 1983;8:199–205.
- [4] Borrmann S, Jaenicke R, Neumann P. On spatial distribution and inter-droplet distances measured in stratus clouds with in-line holography. *Atmos Res* 1998;49:199–212.
- [5] Owen RB, Zozulya AA. In-line digital holographic sensor for monitoring and characterizing marine particulates. *Opt Eng* 2000;39:2187–97.
- [6] Black KS, Sun H, Craig G, Paterson DM, Watson J, Tolhurst T. Incipient erosion of biostabilized sediments examined using particle-field optical holography. *Environ Sci Technol* 2001;35:2275–81.
- [7] Xu L, Miao J, Asundi A. Properties of digital holography based on in-line configuration. *Opt Eng* 2000;39:3214–9.
- [8] Onural L, Scott PD. Digital decoding of in-line holograms. *Opt Eng* 1987;26:1124–32.
- [9] Kreis T, Adams M, Jüptner W. Digital in-line holography in particle measurement. *Proc. SPIE* 1999;3744:54–64.
- [10] Pan G, Meng H. Digital holography of particle fields: reconstruction by use of complex amplitude. *Appl Opt* 2003;42:827–33.

- [11] Onural L, Ozgen MT. Extraction of three-dimensional object-location information directly from in-line holograms using Wigner analysis. *J Opt Soc Am* 1992;A9:252–60.
- [12] Soontaranon S, Widjaja J, Asakura T. Direct analysis of in-line particle holograms by using wavelet transform and envelope reconstruction method. *Optik* 2002;114:489–94.
- [13] Pennebaker WB, Mitchell JL. *JPEG Still Image Data Compression Standard*. New York: Van Nostrand Reinhold; 1993.
- [14] Widjaja J. Effects of image compression on digital specklegrams. *Opt Lasers Eng* 2003;39:501–6.
- [15] Murata K, Fujiwara H, Asakura T. Several problems in in-line Fraunhofer holography for bubble-chamber track recording. In: *Proceedings of Conference on Engineering Use of Holography*, 1970, pp. 289–300.
- [16] Oppenheim AV, Willsky AS. *Signals and Systems*. Upper Saddle River: Prentice-Hall; 1997.
- [17] Yang S, Zhang X, Mitra S. Performance of lossy compression algorithms from statistical and perceptual metrics. In: *Proceedings of 12th IEEE Symposium on Computer-Based Medical Systems*; 1999, pp. 242–247.